Study of Dirac states in HgTe/CdHgTe quantum wells of crystallographic orientation (001)

© Yu.B. Vasilyev

Ioffe Institute,
194021 St. Petersburg, Russia

E-mail: yu.vasilyev@mail.ioffe.ru

Received May 3, 2024
Revised August 4, 2024
Accepted October 30, 2024

Cyclotron resonance in HgTe/HgCdTe (001) quantum wells of various widths is studied using terahertz Fourier transform spectroscopy. From the measurement results, the values of the effective masses of charge carriers and the energies of transitions between Landau levels of several size quantization subbands were obtained. The values of intersubband energies determined from experiments are compared with theoretical values.

Keywords: cyclotron resonance, Fourier spectroscopy, HgTe/HgCdTe quantum wells.

DOI: 10.61011/SC.2024.09.59918.6541A

1. Introduction

A topological insulator is a new state of matter characterized by the presence of a band gap in the volume and gap-free conductive edge or surface states. HgTe/CdHgTe quantum wells are well-studied topological insulators. It was found that a phase transition from a normal insulator to a topological insulator is observed in HgTe/CdHgTe quantum wells when the width of the quantum well exceeds the critical value of $d_c = 6.3$ nm [1]. Studies of cyclotron resonance (CR) in HgTe quantum wells have been described in a large number of papers [2–9]. The main part of such measurements was carried out for quantum wells with crystal orientation (013). No detailed CR studies have been conducted for quantum wells (001), with the exception of quantum wells of critical width [9]. According to theoretical calculations [10], the energy spectra for wells with different crystal orientations should differ markedly, but there is no experimental confirmation of this. CR studies were performed in this paper, from which parameter estimates were obtained for HgTe/CdHgTe wells of various widths with a crystallographic orientation (001).

2. Samples and experimental procedure

The four samples studied in this work (Table 1), were grown by molecular beam epitaxy under the same growth conditions and contain HgTe/$Hg_{0.3}Cd_{0.7}$Te quantum wells with a well width of 6, 7, 8 and 21 nm. The samples have *n*-type of conductivity with carrier concentration in the range of $(1-5)\cdot 10^{11}\,\mathrm{cm}^{-2}$ and mobility of $\sim 10^5\,\mathrm{cm}^2/(\mathrm{V}\cdot\mathrm{s})$. The CR spectra were obtained using a Fourier spectrometer in the spectral range of $20-900\,\mathrm{cm}^{-1}$ using unpolarized light. The sample substrate was ground at an angle of $\sim 3^\circ$ to avoid interference effects. The magnetic field was applied in the direction of the growth of the structures, the measurements are carried out in Faraday geometry at a temperature of 4 K. The absorption spectra were measured with a resolution of $1\,\mathrm{cm}^{-1}$ and normalized to scans at $B = 0$.

3. Results and discussion

The main results of our study are shown in Figures 1 and 2, where the squares show the experimentally measured absorption line energies from the magnetic field for samples with normal and inverted band structures, respectively. Figure 1 shows the dependence of the absorption line energy on the magnetic field for a sample with a well width of 6 nm. The insert shows typical transmission spectra for two values of the applied magnetic field. Only one absorption mode is observed in < 6 T fields, attributed to the electron CR in the HgTe quantum well. The effective mass of the CR energy is determined to be $0.041m_0$, which corresponds to the values indicated in the literature, but much more than the bulk mass of the electron $0.02m_0$. The splitting of the CR line is visible in > 9 T magnetic fields which is associated with transitions between different pairs of Landau levels. Such splitting is typical for two-dimensional electronic systems in narrow-band semiconductor structures characterized by strong nonparabolicity of the conduction band.

Table 1. Parameters of HgTe/CdHgTe quantum wells*

Sample	W	μ	n_{2D}	m
6	6	12.6	2.7	0.041
7	7	10	1.2	0.028
8	8	9.5	1.7	0.025
21	21	61	4	0.019

Note. * QW width W — in nm, mobility — in units $10^4\,\mathrm{cm}^2/(\mathrm{V}\cdot\mathrm{c})$; n_{2D} — $10^{11}\,\mathrm{see}^{-2}$; m — the effective mass of carriers, determined from the CR as m/m_0.

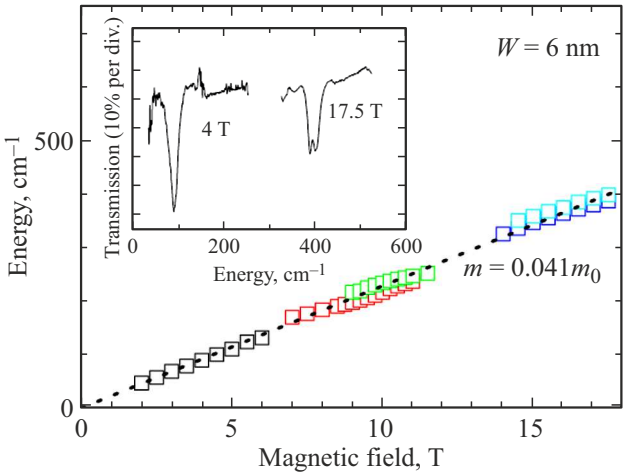

Figure 1. Dependences of the absorption line energy on the magnetic field for a sample 6 with a normal band structure. Experimental data are shown by squares. The dotted line corresponds to the CR of the carriers with an effective mass of $0.041m_0$. The transmittance spectra of sample 6 for magnetic field values of 4 and 17.5 T are shown in the insert.

More complex absorption spectra are observed for samples with an inverted band structure. The dependences of the absorption line energy on the magnetic field are shown in Figure 2 for three samples with a well width of 7, 8 and 21 nm. All three samples demonstrate qualitatively similar dependences of the absorption line energy on the magnetic field. The spectra consist of several (more than two) clearly different modes. The initial part (for magnetic fields up to 5–6 T) of the graphs in Figure 2 is a CR line passing through the origin and characterized by a linear dependence of energy on the magnetic field. The CR line loses its intensity with an increase of the magnetic field and it disappears in the fields of > 6 T. Instead, new mods of a different nature appear. They are also linear relative to the magnetic field, but shifted in energy relative to the line passing through the origin. The energy separation between such absorption modes seems to be independent of the field, and the modes run approximately parallel to each other as the magnetic field increases.

The effective carrier masses, determined by the slope of the lines, are shown in the graphs in Figure 2 and in Table 1.

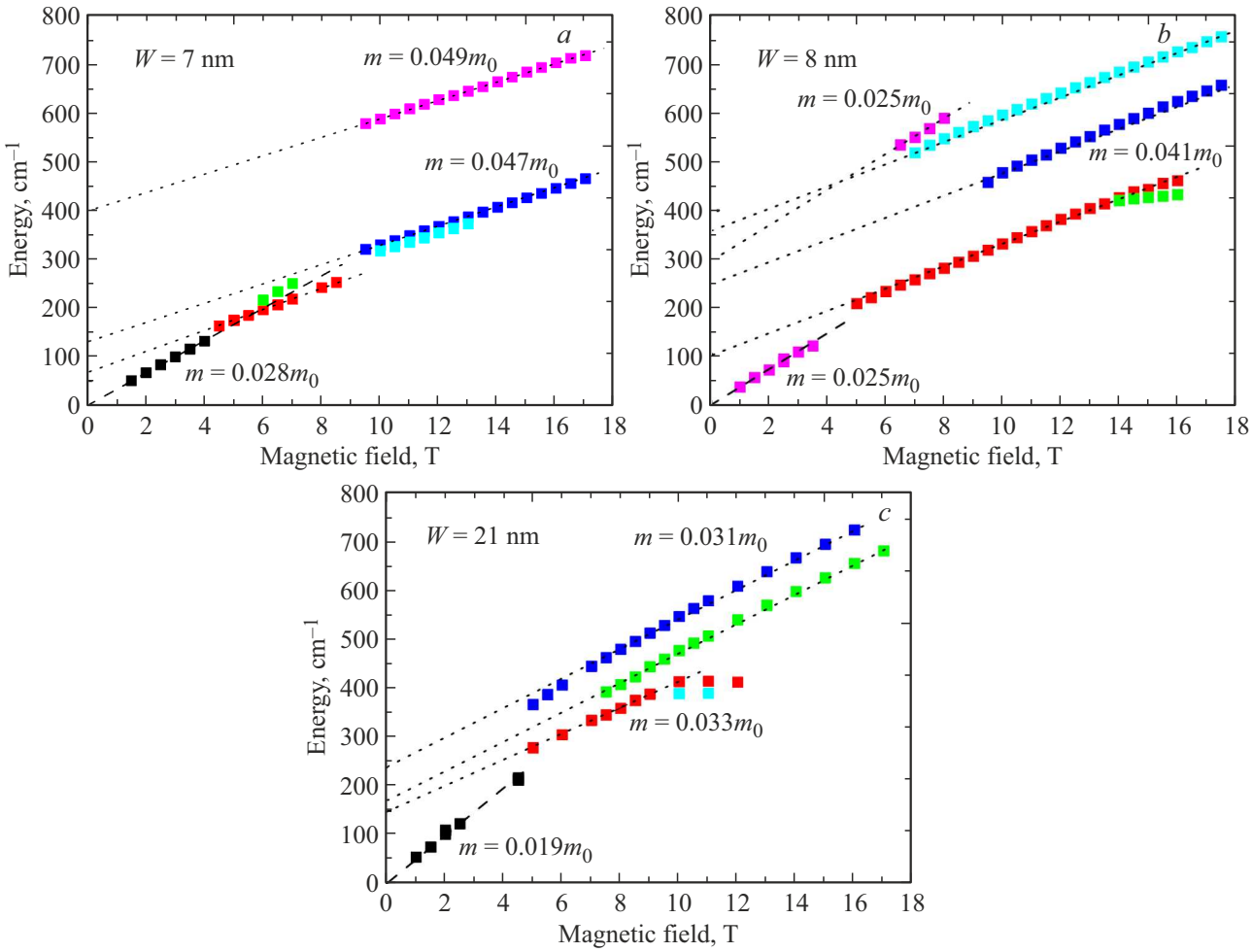

Figure 2. Dependences of the energy of absorption lines on the magnetic field for samples with an inverted band structure. Experimental data are shown by squares. The symbols corresponding to the transitions between levels with the same slope in the magnetic field are filled with identical (purple) color for sample 8. The dashed and dotted lines show the energies of the CR and interband transitions: *a* — for sample 7, *b* — for sample 8, *c* —for sample 21.

Table 2. Interband energies in HgTe/CdHgTe quantum wells, obtained from fitting experimental data and calculated [11]

QW width, nm	$E1-H1$	$E1-H2$	$H1-H2$	$H1-H3$	$H1-H4$	$P1$	$P2$	$P3$
	Calculation, meV					Experiment, meV		
6	4	71	67				4	
7	18	33	51			50	16	9
8	36	7	43			45	31	13
21	86	83	3	6	9	29	21	18

The dependence of the mass of charge carriers on the width of the well is clearly visible. The effective mass in the wide well (21 nm) is $0.019m_0$, which approximately coincides with the effective mass of electrons in the bulk HgTe ($0.02m_0$). This indicates that the carriers in our samples are electrons. High-frequency complementary modes are of particular interest. The dependence of the energies of these modes on the magnetic field differs from the behavior of cyclotron resonance. The rest of this study is devoted to the study of the features of these modes.

The dependencies in strong fields in Figure 2 (point curves) can be described by the linear equation $E(B) = P + AB/m$ with two fitting parameters $P\,(\mathrm{cm}^{-1})$ and m (as part of m_0). Within the limits of the accuracy of the fit, the obtained effective mass value is obviously not equal to the value measured directly by CR in weak magnetic fields. Even if we take into account the non-parabolicity of the conduction band, high-frequency modes can hardly be explained by the absorption of CR inside one subband. The observed features of these modes indicate that they are caused by transitions between Landau levels belonging to different subbands. The electron quantization energy increases as the magnetic field increases and the filling of the levels of various subbands changes, and as a result, charge carriers are redistributed between them, making it possible to make higher-energy transitions in case of the light absorption. This means that additional modes become visible with an increase of the magnetic field, when higher-energy states are emptied. The energies of the interband transitions were estimated by extrapolating the measured energy dependences to $B = 0$, and the results are shown in Table 2. Theoretically calculated [11] values of energy distances between different subbands are also presented in Table 2. Experimentally determined interband energies $H1-E1$ and $H2-H1$, where the indices H and E denote hole and electronic states, respectively, are consistent with the theoretically calculated values [11] for samples 6, 7 and 8. As can be seen from Table 2, the measured energy of the line $P2$ for samples 6, 7, and 8 is in good agreement with the calculated energy of the transitions $E1-H1$, and the line $P1$ corresponds to the transitions $H1-H2$ for samples 7 and 8. The calculated energy values of the subbands for sample 21 were obtained by extrapolating the data from paper [11].

4. Conclusion

The values of the effective masses of charge carriers and the energy of transitions between Landau levels of several subbands of dimensional quantization are obtained from the results of measurements of cyclotron resonance in HgTe/HgCdTe (001) quantum wells, which are consistent with the theoretically calculated values for wells with a width of 6–8 nm.

Conflict of interest

The authors declare that they have no conflict of interest.

References

[1] S.A. Tarasenko, M.V. Durnev, M.O. Nestoklon, E.L. Ivchenko, J.-W. Luo, A. Zunger. Phys. Rev. B, **91** (8), 081302(R) (2015).
[2] A.V. Ikonnikov, M.S. Zholudev, K.E. Spirin, A.A. Lastovkin, K.V. Maremyanin, V.Y. Aleshkin, V.I. Gavrilenko, O. Drachenko, M. Helm, J. Wosnitza, M.Goiran. Semicond. Sci. Technol., **26** (12), 125011 (2011).
[3] D.A. Kozlov, Z.D. Kwon, N.N. Mikhailov, S.A. Dvoretsky, J.C. Portal. Pisma ZhETF, **93** (3), 186 (2011). (in Russian).
[4] M. Zholudev, F. Teppe, M. Orlita, C. Consejo, J. Torres, N. Dyakonova, M. Czapkiewicz, J. Wróbel, G. Grabecki, N. Mikhailov, S. Dvoretskii. Phys. Rev. B, **86** (20), 205420 (2012).
[5] A.A. Greshnov, Y.B. Vasiliev, N.N. Mikhailov, G.Y. Vasilieva, D. Smirnov. Pisma ZhETF, **97** (2), 108 (2013) (in Russian).
[6] J. Ludwig, Y.B. Vasilyev, N.N. Mikhailov, J.M. Poumirol, Z. Jiang, O. Vafek, D. Smirnov. Phys. Rev. B, **89** (24), 241406 (2014).
[7] A.M. Shuvaev, V. Dziom, N.N. Mikhailov, Z.D. Kvon, Y. Shao, D.N. Basov, A. Pimenov. Phys. Rev. B, **96** (15), 155434 (2017).
[8] A. Shuvaev, V. Dziom, J. Gospodarič, E.G. Novik, A.A. Dobretsova, N.N. Mikhailov, Z.D. Kvon, A. Pimenov. Nanomaterials, **12** (14), 2492 (2022).
[9] M. Orlita, K. Masztalerz, C. Faugeras, M. Potemski, E.G. Novik, C. Brü ne, H. Buhmann, L. W. Molenkamp. Phys. Rev. B, **83** (11), 115307 (2011).
[10] M.V. Durnev, G.V. Budkin, S.A. Tarasenko. ZhETF, **162** (4), 570 (2022). (in Russian).
[11] M. Konig, H. Buhmann, L.W. Molenkamp, T. L. Hughes, C.-X. Liu, X.L. Qi, S.C. Zhang. J. Phys. Soc. Jpn., **77**, 031007 (2008).

Translated by A.Akhtyamov